THE JOURNAL OF BIOLOGICAL CHEMISTRY VOL. 287, NO. 12, pp. 8986–8993, March 16, 2012

Luminal and Cytosolic pH Feedback on Proton Pump Activity and ATP Affinity of V-type ATPase from *Arabidopsis*[*S]

Received for publication, October 4, 2011, and in revised form, December 19, 2011 Published, JBC Papers in Press, January 3, 2012, DOI 10.1074/jbc.M111.310367

Florian Rienmüller[‡], Ingo Dreyer[§1], Gerald Schönknecht[¶], Alexander Schulz[‡], Karin Schumacher[‖], Réka Nagy[**], Enrico Martinoia[**], Irene Marten[‡], and Rainer Hedrich[‡ ‡‡2]

From the [‡]University of Würzburg, Institute for Molecular Plant Physiology and Biophysics, Julius-von-Sachs Platz 2, D-97082 Würzburg, Germany, [§]Centro de Biotecnologia y Genomica de Plantas, Universidad Politécnica de Madrid, Plant Biophysics, Campus de Montegancedo, Carretera M-40, km 37.7, 28223 Pozuelo de Alarcón (Madrid), Spain, the [¶]Department of Botany, Oklahoma State University, Stillwater, Oklahoma 74078, the [‖]Heidelberg Institute for Plant Sciences, University of Heidelberg, Im Neuenheimer Feld 360, 69120 Heidelberg, Germany, the [**]Institute of Plant Biology, University of Zürich, Zollikerstrasse 107, Zurich, Switzerland, and [‡‡]King Saud University, Riyadh 11451, Saudi Arabia

Background: Vacuolar H^+-ATPases use ATP to generate a transmembrane proton motive force.
Results: Cytosolic and vacuolar pH affect proton transport rate and ATP binding of V-ATPases.
Conclusion: With decreasing pH, the dissociation of transported protons from V-ATPase seems to be hindered.
Significance: V-ATPase activity is optimized according to existing H^+ concentrations via close coupling between the ATP-binding and proton-translocating complex.

Proton pumping of the vacuolar-type H^+-ATPase into the lumen of the central plant organelle generates a proton gradient of often 1–2 pH units or more. Although structural aspects of the V-type ATPase have been studied in great detail, the question of whether and how the proton pump action is controlled by the proton concentration on both sides of the membrane is not understood. Applying the patch clamp technique to isolated vacuoles from *Arabidopsis* mesophyll cells in the whole-vacuole mode, we studied the response of the V-ATPase to protons, voltage, and ATP. Current-voltage relationships at different luminal pH values indicated decreasing coupling ratios with acidification. A detailed study of ATP-dependent H^+-pump currents at a variety of different pH conditions showed a complex regulation of V-ATPase activity by both cytosolic and vacuolar pH. At cytosolic pH 7.5, vacuolar pH changes had relative little effects. Yet, at cytosolic pH 5.5, a 100-fold increase in vacuolar proton concentration resulted in a 70-fold increase of the affinity for ATP binding on the cytosolic side. Changes in pH on either side of the membrane seem to be transferred by the V-ATPase to the other side.

A mathematical model was developed that indicates a feedback of proton concentration on peak H^+ current amplitude (v_{max}) and ATP consumption (K_m) of the V-ATPase. It proposes that for efficient V-ATPase function dissociation of transported protons from the pump protein might become higher with increasing pH. This feature results in an optimization of H^+ pumping by the V-ATPase according to existing H^+ concentrations.

Among the F-, A-, and V-type family of ATP synthases and ATPases, the best characterized member is the F_oF_1-ATP synthase (for review, see Ref. 1). It consists of a F_o and a F_1 complex, which differ in their physicochemical and functional properties. During interconversion between energy stored in an electrochemical proton gradient and chemical energy stored in ATP, the hydrophilic F_1 domain binds ATP, and the membrane-embedded hydrophobic F_o complex mediates translocation of protons across the membrane. ATP hydrolysis in F_1 can drive transmembrane H^+ transport in F_o against an electrochemical potential gradient, or an existing proton motive force can be used to synthesize ATP, as in photophosphorylation and oxidative phosphorylation. For coupling proton transport to ATP synthesis/hydrolysis, the F_o and F_1 domains function as rotary motors (2), which are coupled by elastic mechanical power transmission (3). To function primarily as a synthase, it was proposed that the H^+/ATP coupling ratio *c* reflecting the interconversion of the energy stored in the electrochemical gradient into ATP should be ~4. Thus, the consumption of more protons per ATP synthesized would assure the maintenance of a high phosphorylation potential (2). Instead, a smaller coupling value (~2) would be preferable when the enzyme acts as an ATPase. If fewer protons were pumped per hydrolyzed ATP, a larger electrochemical gradient would be maintained (2).

During the evolution of proton-translocating F_oF_1 complexes, at least two functional conversions have probably occurred with one leading first from an ancestral ATPase of an anaerobe to an ATPase in prokaryotes followed by the transformation of some ATP synthases to endomembrane/vacuolar ATPases (2, 4). The latter functional transition appears to be related to a duplication and fusion of the gene encoding the c subunit within the F_o complex and loss of proton-binding car-

* This work was supported by Deutsche Forschungsgemeinschaft Grants FOR1061 and GK1342 (to R. H.) and GK1342 (to I. M.).
[S] This article contains a supplemental Appendix and supplemental Fig. 1.
[1] To whom correspondence may be addressed: Centro de Biotecnologia y Genomica de Plantas, Universidad Politécnica de Madrid, Plant Biophysics, Campus de Montegancedo, Carretera M-40, km 37.7, 28223 Pozuelo de Alarcón (Madrid), Spain. Tel.: 34-91-336-4588; E-mail: ingo.dreyer@upm.es.
[2] To whom correspondence may be addressed: Institute for Molecular Plant Physiology and Biophysics, University of Würzburg, Julius-von-Sachs Platz 2, D-97082 Würzburg, Germany. Tel.: 49-931-3186100; E-mail: hedrich@botanik.uni-wuerzburg.de.

boxylates in amino acids of the c subunit (2). This notion is partially supported by the fact that some ATP synthases from anaerobic Archaea, *e.g. Archaeoglobus fulgidus* or *Methanothermobacter thermoautotrophicus*, are characterized by double-sized c subunits (4–6). With further bisection of the H^+/ATP coupling ratio from 4 to 2 for the change in primary function from an ATP synthase to an ATPase, the electroenzymes optimize performance in response to thermodynamics, given by the unique environments of the host organelle in question (*e.g.* chloroplasts for ATP synthases *versus* vacuoles for ATPases).

During photophosphorylation, the pH of the thylakoid lumen acidifies without strong polarization of the photosynthetic membrane. ATP synthases that function in photophosphorylation in chloroplasts thus predominately use the proton gradient of the proton motive force for ATP formation. Instead, under physiological conditions the vacuolar ATPase uses the chemical energy of ATP to pump protons into the lumen of the central plant organelle. As a result, a pH gradient, in the order of 1 to 2 pH units and more, and an electrical field across the vacuolar membrane are generated. The latter, however, is only weak (7, 8) because of compensatory counterbalancing ion fluxes. The proton motive force provides a versatile energy store that can be used on demand to *e.g.* accumulate metabolites such as sugars in antiport with protons (9). Under experimental conditions, when in patch clamp studies, a cytosol-directed pH gradient was established, and ADP and P_i was present at the cytosolic side of isolated vacuoles, the V-ATPase can also work as an ATP synthase (10, *cf.* Refs. 11 and 12).

The V-type ATPase operates as an H^+-pumping ATPase under physiological conditions. At luminal proton concentrations differing from cytosolic ones by an order of magnitude or more, proper electroenzyme function should require a feedback via changes in luminal and cytosolic pH. Therefore, to gain insights in the pH dependence of the V-ATPase, here, we performed patch clamp experiments with isolated vacuoles from mesophyll cells of the model plant *Arabidopsis*. Proton pump kinetics and current-voltage relationships were obtained from whole-vacuole recordings in the presence and absence of ATP under defined cytoplasmic and vacuolar pH.

EXPERIMENTAL PROCEDURES

Plant Material and Vacuole Isolation—Growth conditions of *Arabidopsis thaliana* ecotype Columbia (Col-0), *det3-1*, *vha-a2 vha-a3*, and *tpc1-2* mutant were as described previously (9) According to Ref. 13, mesophyll cell protoplasts were isolated for subsequent release of the vacuoles via treatment with a hypotonic solution (10 mM EGTA, 10 mM HEPES/Tris, pH 7.5, osmolality of 200 mosmol kg^{-1} adjusted with D-sorbitol).

Electrophysiology—Following the convention for electrical measurements on endomembranes (14), patch clamp experiments on vacuoles were performed in the whole-vacuole configuration as described previously (9, 15). An EPC7 or EPC10 patch clamp amplifier (HEKA) was used for macroscopic current recordings from mesophyll cell vacuoles at a data acquisition rate of 2 ms (EPC7), 10 ms, or 100 μs (EPC10). After macroscopic currents were low pass-filtered at 30 Hz (EPC7) or 100 Hz (EPC10), data were digitized by an ITC-16 (EPC7) (Instrutech Corp.) or the integral LIH8+8 of the EPC10 (HEKA). The data were stored on Windows environment computers. The clamped voltages were corrected for the liquid junction potentials (16). Different software such as Pulse, Patchmaster (HEKA), and IGOR PRO (Wave Metrics, Inc.) were used for data acquisition and offline analysis. Macroscopic currents were normalized to membrane capacitance (C_m) of the respective vacuole to allow quantitative comparison of the proton transport capacity among different vacuoles. The holding potential for V-ATPase measurements was usually set to 0 mV if not otherwise stated. Voltage ramps (1 mV/ms) were applied in a range either between −180 mV and 100 mV within 270 ms or between −250 mV to 100 mV within 340 ms.

Patch Clamp Solutions—Symmetrical bath and pipette solutions were used generally composed of 100 mM KCl, 5 mM $MgCl_2$, and 1 mM $CaCl_2$. The media were adjusted to an osmolality of 400 mosmol kg^{-1} with D-sorbitol. pH values were adjusted to pH 7.5 and 6.5 with 10 mM HEPES/Tris, to pH 5.5 with 10 mM MES/Tris, or to pH 9.5 with 10 mM Bis-Tris propane/MES. Mg-ATP (Sigma) was added from an ATP stock solution to the bath medium facing the cytosolic side of the vacuolar membrane. The ATP-free bath solution was replaced by the ATP-containing one either upon bath perfusion in the recording chamber or via an application pipette in front of the respective vacuole (9). Variations in the composition of the solutions are given in the figure legends.

Dependence of Coupling Ratio c on Vacuolar pH—The coupling ratio c is defined as number of protons translocated per hydrolyzed ATP molecule. If the pump is coupled tightly and if parallel ionic conductivities are negligible, the generalized pump reaction,

$$c[H^+]_{cyt} + [ATP] \rightleftarrows c[H^+]_{vac} + [ADP] + [P_i] \qquad \text{(Eq. 1)}$$

is at equilibrium at the transmembrane voltage E_{rev} (17, 18),

$$E_{rev} = \frac{RT}{cF} \cdot \ln \frac{[ADP]\cdot[P_i]\cdot[H^+]^c_{vac}}{K_{ATP}\cdot[ATP]\cdot[H^+]^c_{cyt}} \qquad \text{(Eq. 2)}$$

where K_{ATP} is the apparent equilibrium constant for ATP hydrolysis; R, T, and F have their usual meanings; c is the coupling ratio; brackets represent chemical concentrations of the reactants; and the indices vac and cyt denote the vacuolar and cytosolic compartments, respectively. Under constant cytosolic conditions, the unknown value,

$$E_{ATP} = RT/F \cdot \ln[([ADP]\cdot[P_i])/(K_{ATP}\cdot[ATP])] \qquad \text{(Eq. 3)}$$

is constant. Therefore, the relative change of the coupling ratio r_c upon changes in vacuolar pH can be calculated as follows.

$$r_{c,1\rightarrow 2} = \frac{c_2}{c_1} = \frac{E_{rev,pHvac1} - 2.303\cdot\frac{RT}{F}\cdot(pH_{cyt} - pH_{vac1})}{E_{rev,pHvac2} - 2.303\cdot\frac{RT}{F}\cdot(pH_{cyt} - pH_{vac2})} \qquad \text{(Eq. 4)}$$

RESULTS

ATP-powered V-ATPase Currents and Polarization of Vacuolar Membrane—The V-type ATPase interconverts metabolic energy and electrochemical proton gradient. Although its structure and biological role becomes increasingly well understood (Ref. 19 and references cited therein), their quantitative electrochemical function and regulation is not yet fully understood. To gain insight into this issue, in our patch clamp analysis, we focused on the model plant *A. thaliana*. Following isolation of mesophyll cell protoplasts, vacuoles were liberated on demand directly in the patch clamp chamber upon selective osmotic swelling and rupture of the plasma membrane (15, 20). To record ATPase-mediated currents from the entire V-type proton pump population, the whole vacuole configuration was established applying a short high voltage pulse in the vacuole-attached mode. As a result, the membrane patch under the patch pipette was broken allowing equilibration of the vacuole lumen with the pipette electrolyte solution (9). Under this condition, proton currents associated with ATP hydrolysis were recorded. The V-ATPase population was activated upon ATP application on the cytoplasmic side of the vacuolar membrane via perfusion pipettes (9, 20) or bath perfusion. Different experimental conditions under which competing transport processes did not take place or were largely reduced were used for recording of the ATP-induced proton currents. To minimize or even eliminate interfering background current components such as the slow vacuolar (TPC1) channels, ATP-induced pump currents were monitored at zero membrane voltage under symmetrical ionic conditions and defined cytoplasmic and vacuolar pH. When the proton pumps of vacuoles were challenged with 5 mM ATP and pH buffered to symmetrical pH 7.5 in the bath and patch pipette, outward currents of ~2.5 pA/pF were measured (Fig. 1*A*). To test whether these currents were indeed mediated by ATP-activated V-ATPases, the specific V-ATPase inhibitor bafilomycin (500 nM) was added to the bath solution as soon as the steady-state level in proton pump activity was reached. In the presence of bafilomycin the ATP-dependent currents ceased (Fig. 1*A*). In addition, the V-ATPase-dependent ability for membrane polarization was tested in the current clamp mode. With cytosolic pH 6.5 and luminal pH 7.5, proton pumps powered by 5 mM ATP hyperpolarized the vacuolar membrane potential by −72.4 mV in wild type and −3 mV in the V-ATPase-deficient mutant *vha-a2 vha-a3* (Fig. 1*B*) (19).

V-ATPase Proton Pumping Requires VHA-a and -C Subunits—V-ATPases consist of two domains with different structure and function. The peripheral ATP-hydrolyzing V_1 complex is composed of eight subunits (VHA-A to -H), whereas the integral V_0 complex contains six subunits (VHA-a, -c, -c′, -c″, -d, and -e) and is engaged with proton translocation (21). Recently, we demonstrated that the double mutant *vha-a2 vha-a3* lacks V-ATPase-mediated ATP hydrolysis and proton currents (19). To test the effect of changes in the peripheral V_1 complex on V-ATPase activity, in a similar approach, we analyzed vacuoles from the *det3-1* mutant. In the *det3* mutant, a Thr→Ala mutation in an intron of the subunit C-encoding the *VHA-C* gene causes reduced mRNA levels leading to lower VHA-C protein levels and reduced V-ATPase activity (22). When compared with the situation in wild type (100%), pump currents in *det3-1* vacuoles with 5 mM ATP were reduced by ~62% (supplemental Fig. 1, *A* and *B*). This drop in proton pump currents corresponds well to a previously reported 60% decrease in V-ATPase activity in the *det3* mutant (22). Because the protein level of subunit c within the V_0 complex, however, was unaltered in the *det3* mutant (22), the results are in line with the notion that the ATP-hydrolyzing V_1 complex is essential for the proton transport via the membrane-spanning V_0 complex.

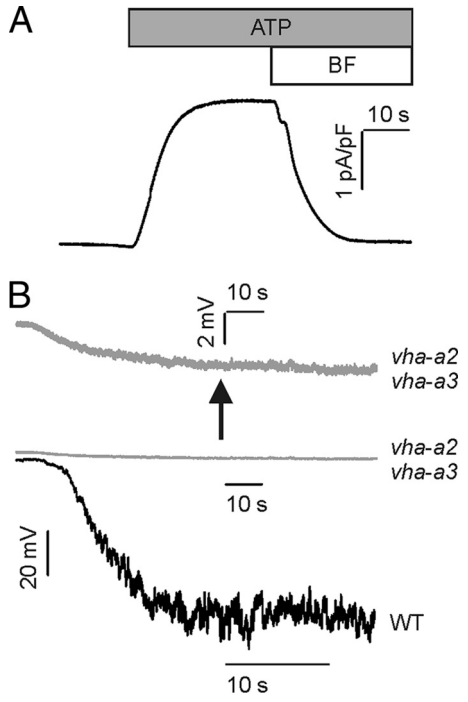

FIGURE 1. **ATP-dependent activation of V-ATPase-mediated proton currents in mesophyll vacuoles from *A. thaliana*.** *A*, outward currents were evoked upon application of 5 mM ATP to the bath solution. These ATP-induced currents vanished upon the additional application of bafilomycin (*BF*, 500 nM), indicating that they represent V-ATPase-mediated proton currents. *Bars above* the current trace in *A* indicate the presence of ATP ± bafilomycin during current recording. The experiments in *A* were performed under symmetrical ionic conditions at pH of 7.5. *B*, membrane polarization of WT and *vha-a2 vha-a3* mesophyll vacuoles. The ATP-induced (5 mM) proton pump activity resulted in an increase of the tonoplast voltage up to −72.4 mV for WT (*black trace*) and −3 mV in the double mutant (*gray traces*) as indicated by the downward deflection of the voltage traces. The topmost trace represents a close-up of the *middle* one. Current clamp experiments in *B* were performed under balanced ionic conditions of 50 mM KCl at pH_{cyt} 6.5/pH_{vac} 7.5.

Coupling Ratio Is pH-dependent—An ideal coupling ratio *c* of two protons pumped for each hydrolyzed ATP molecule was proposed for V-ATPases (2). Early studies on V-ATPases found a stoichiometry of 2 (23–25), but later reports claimed variable coupling ratios with up to 4 protons being transferred for each ATP hydrolyzed by the vacuolar proton pump (17, 18, 26, 27). It was hypothesized that the coupling ratio *c* depends on the proton concentration at both sides of the tonoplast and the membrane voltage (17, 28). To address this issue, we determined the proton pump activity of the V-ATPase as a function of pH and membrane voltage. To avoid superimposition of the ATP-evoked pump currents by voltage-dependent slow vacuolar

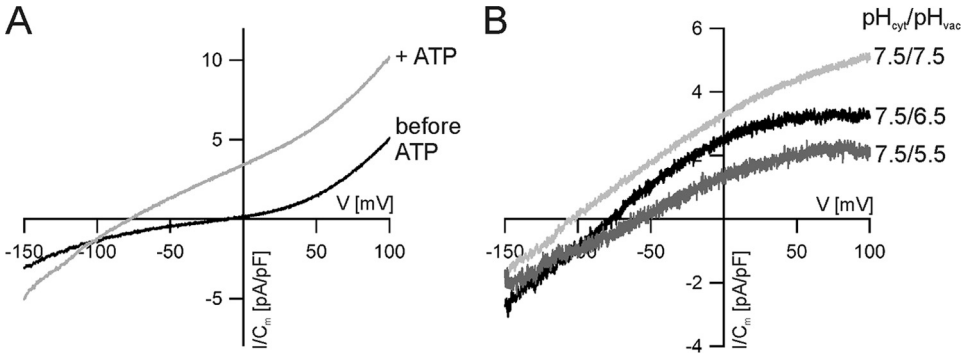

FIGURE 2. **Voltage dependence of the V-ATPase in *tpc1-2* mesophyll vacuoles.** *A*, the macroscopic current response of an individual vacuole to a voltage ramp in the range of −150 mV to +100 mV before (*black*) and after (*gray*) addition of 5 mM ATP under symmetrical pH 7.5 is shown. The intersection of both curves provided the reversal potential of the electroenzyme. Each current-voltage curve (*I*(*V*)) represents the average of five *I*(*V*) values recorded from the same vacuole. *B*, representative voltage-dependent net H^+ pump currents determined in the presence of pH 7.5 in the cytosol and three different vacuolar pH values are shown. The net pump currents were obtained by subtracting the averaged *I*(*V*) curve (shown in *A* for pH_{vac} 7.5) recorded in the absence of ATP from that in the presence of ATP. The net pump currents under symmetrical pH 7.5 presented in *B* were derived from the *I*(*V*) curves given in *A*. The ionic conditions were equivalent to *A* except that the vacuolar pH was adjusted either to pH 7.5 (*light gray*), pH 6.5 (*black*), or pH 5.5 (*dark gray*). The reversal potentials were $E_{rev(pHvac7.5)} = -94.5 \pm 14.0$ mV ($n = 5$), $E_{rev(pHvac6.5)} = -67.5 \pm 10.6$ mV ($n = 5$), and $E_{rev(pHvac5.5)} = -49.6 \pm 3.9$ mV ($n = 3$). The experiments in *A* and *B* were performed with symmetrical solutions containing 50 mM CsCl and without calcium.

(TPC1) channel-mediated cation currents, the patch clamp experiments were conducted with vacuoles isolated from the TPC1-loss-of-function mutant *tpc1-2* (29, 30). Furthermore, potassium-selective channels of the TPK1-type (31) were blocked by substituting K^+ with Cs^+ in the patch clamp solutions (32). Under defined cytoplasmic and vacuolar pH, the response of an individual vacuole to voltage ramps (1 mV/ms) was recorded prior to and after ATP application. An example of the macroscopic current-voltage relationships evoked by voltage ramps in the range from −150 to +100 mV in the absence and presence of 5 mM ATP at symmetrical pH 7.5 is shown in Fig. 2*A*. When the current-voltage (*I*/*V*) curve recorded in the absence of ATP was subtracted from the one obtained with ATP, the deduced ionic currents reflect the voltage behavior of the V-ATPase (Fig. 2*B*). In the absence of a pH gradient across the vacuolar membrane, ATP-induced proton currents changed direction at average at -94.5 ± 14.0 mV ($n = 5$). After an increase in the vacuolar proton concentration by a factor of 10 (pH_{cyt} 7.5/pH_{vac} 6.5),[3] the V-ATPase had to transport protons against a gradient. Accordingly, proton currents at zero membrane voltage dropped in average from 2.9 ± 0.3 pA/pF ($n = 5$) to 1.9 ± 0.1 pA/pF ($n = 5$), and the reversal potential of the pump currents shifted from −94.5 mV to -67.5 mV $\pm$ 10.6 mV ($n = 5$) (Fig. 2*B*). At a 100-fold gradient (pH_{cyt} 7.5/pH_{vac} 5.5), proton currents at zero membrane voltage further decreased to 1.1 ± 0.1 pA/pF and currents reversed in average at -49.6 ± 3.9 mV ($n = 3$) (Fig. 2*B*). From these values, we calculated that the H^+/ATP coupling ratio decreased by ~25% (r_c 7.5→6.5 = 0.75 ± 0.17) upon a change from pH_{vac} 7.5 to pH_{vac} 6.5. An additional 10-fold increase in the vacuolar proton concentration (pH_{cyt} 7.5/pH_{vac} 5.5) had a similar effect. The coupling ratio decreased by another ~25% (r_c 6.5→5.5 = 0.75 ± 0.08).

[3] The abbreviations used are: pH_{cyt}, cytosolic pH; pH_{vac}, vacuolar pH; E_{rev}, reversal potential.

V-ATPase Proton Transport Capacity, K_m Value, and ATP Hydrolysis Are pH-dependent—The pH-dependent function of the proton pump was further quantified on the basis of steady-state proton currents. With the membrane potential clamped to zero mV and symmetrical cytosolic pH 7.5, a peak steady-state proton-current amplitude of 2.4 ± 0.1 pA/pF was registered from wild type vacuoles in the presence of 5 mM ATP (Fig. 3, *A* and *B*). These pump currents only slightly changed when the luminal pH was changed from pH_{vac} 7.5 to 5.5 (1.8 ± 0.4 pA/pF) or 9.5 (2.2 ± 0.8 pA/pF) (Fig. 3*B*). Unlike the luminal pH, the cytosolic proton concentration in the living plant cell only varies within a small range. However, to drive the V-type ATPase to its limit, the function of the proton pump fueled by 5 mM ATP was additionally studied at a cytosolic pH of 5.5 or 9.5. A cytosolic alkaline shift from pH_{cyt} 7.5 to 9.5 (pH_{vac} 7.5) resulted in a pronounced decrease in V-ATPase-generated proton currents from 2.4 to 0.3 ± 0.1 pA/pF (Fig. 3*B*). Interestingly, these pump current amplitudes were much smaller than under pH_{cyt} 7.5/pH_{vac} 5.5, even though the direction and magnitude of the pH gradient were the same under these two pH conditions. A cytosolic acidification to pH_{cyt} 5.5 (pH_{vac} 7.5) resulted in an increase of pump currents from 2.4 to 3.2 ± 0.1 pA/pF (Fig. 3*B*). Finally, at pH_{cyt} 5.5, the luminal pH was altered from 7.5 to 5.5, and as a result, the pump current at 5 mM ATP was reduced in amplitude by 56% (to 1.4 ± 0.4 pA/pF).

Next, we asked the question whether the observed changes in current amplitudes (Fig. 3) were caused by alterations in ATP affinity or maximum transport capacity of the V-ATPase. For this, we compared the following four pH conditions: symmetrical pH 7.5, symmetrical pH 5.5, physiological pH gradient (pH_{cyt} 7.5/pH_{vac} 5.5), and inverted pH gradient (pH_{cyt} 5.5/pH_{vac} 7.5). When the ATP concentration was increased stepwise up to 10 mM, peak proton pump currents raised following a saturation-type concentration dependence. Fitting a Michelis-Menten function to the saturation curve for symmetrical $pH_{cyt/vac}$ 7.5 revealed a maxi-

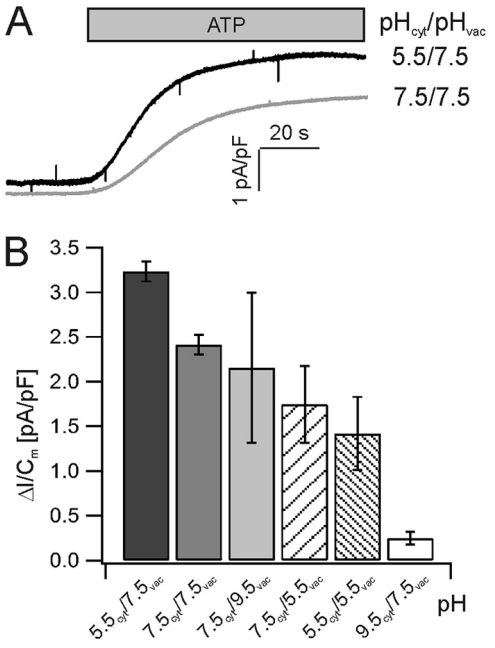

FIGURE 3. **Representative ATP-induced wild-type V-ATPase outward currents.** *A*, application of 5 mM ATP resulted in an increase of proton outward currents given by an upward deflection of the current baseline. Current traces were recorded at 0 mV under symmetrical pH 7.5 or pH$_{cyt}$ 5.5/pH$_{vac}$ 7.5. *B*, V-ATPase outward currents in response to 5 mM ATP under different pH conditions are shown. The number of experiments was from *left* to *right* (n = 3, 6, 4, 4, 3, 6). *Error bars* represent the S.E.

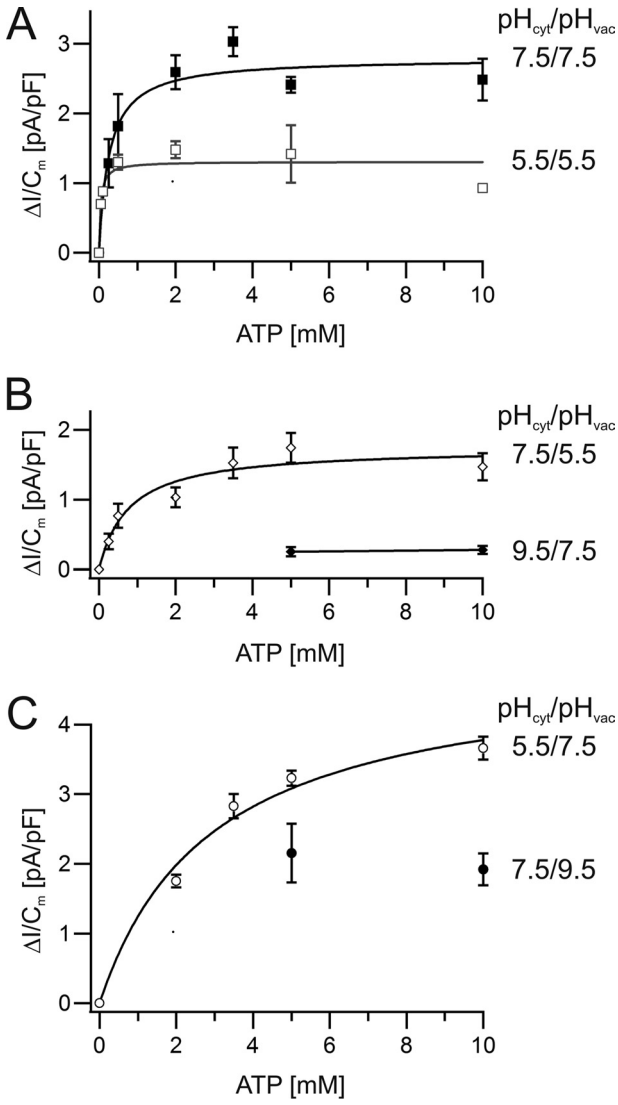

FIGURE 4. **pH dependence of the V-ATPase activity at various ATP levels.** Macroscopic proton pump currents from wild-type vacuoles in response to different ATP concentrations were measured and plotted against the respective ATP concentration. *Solid curves* represent the fit of the data points with a Michaelis-Menten function providing the parameters v_{max} and K_m. The number of experiments were n = 3–6. *Error bars* represent the S.E. *A*, balanced pH values. *Filled squares* show pH$_{cyt}$ 7.5/pH$_{vac}$ 7.5 with v_{max} = 2.8 pA/pF and K_m = 0.3 mM. *Open squares* represent pH$_{cyt}$ 5.5/pH$_{vac}$ 5.5 with v_{max} = 1.3 pA/pF and K_m = 0.04 mM. *B*, cytosol-directed pH gradient. *Open diamonds* indicate pH 7.5$_{cyt}$/5.5$_{vac}$ with v_{max} = 1.7 pA/pF and K_m = 0.8 mM. *Closed diamonds* represent pH$_{cyt}$ 9.5/pH$_{vac}$ 7.5 with $v_{max} \approx$ 0.3 pA/pF. *C*, vacuolar-directed pH gradient. *Open circles* represent pH$_{cyt}$ 5.5/pH$_{vac}$ 7.5 with v_{max} = 4.9 pA/pF and K_m = 2.9 mM. *Filled symbols* describe pH$_{cyt}$ 7.5/pH$_{vac}$ 9.5 with $v_{max} \approx$ 2 pA/pF.

mal proton transport capacity (v_{max}) of 2.8 pA/pF and a K_m value of 0.3 mM (Fig. 4*A*). When the pH gradient was directed into the cytosol (pH$_{cyt}$ 7.5/pH$_{vac}$ 5.5), v_{max} dropped to 1.7 pA/pF, whereas the K_m value was 0.8 mM (Fig. 4*B*). Upon inversion of the pH gradient (pH$_{cyt}$ 5.5/pH$_{vac}$ 7.5), proton currents did not saturate with 10 mM ATP (Fig. 4*C*). However, fitting a saturation curve to the latter data set allowed us to calculate a v_{max} of 4.9 pA/pF and a K_m value of 2.9 mM. Finally, we tested how the pump would respond to cytosolic acidification. Therefore, we buffered both the vacuole lumen and bath solution to pH 5.5 and studied the ATP dependence of proton pumping. Under these extreme cytosolic conditions (pH$_{cyt/vac}$ 5.5), v_{max} was 1.3 pA/pF, comparable with v_{max} at pH$_{cyt}$ 7.5/pH$_{vac}$ 5.5 (1.7 pA/pF), but by a factor of 4 lower to that at pH$_{cyt}$ 5.5/pH$_{vac}$ 7.5. At symmetrical pH 5.5, the K_m value dropped to 0.04 mM, almost two orders of magnitude (*i.e.* 70-fold) lower compared with pH$_{cyt}$ 5.5 and pH$_{vac}$ 7.5 (Fig. 4), whereas at a vacuolar pH of either 7.5 or 5.5, a 100-fold change in proton concentration on the cytosolic side changed the K_m values 10- or 20-fold, respectively, only (Fig. 4). Thus, in line with the 5 mM ATP-powered proton current amplitudes (Fig. 3*B*), the effect of luminal acidification on v_{max} and K_m was much higher in the presence of pH$_{cyt}$ 5.5 than pH$_{cyt}$ 7.5. Providing the V-ATPase with high ATP-affinity pumping at pH$_{vac}$ 5.5 might help the cell to recover from cytosolic acidification.

Modeling Pump Kinetics—To understand the behavior of the pump (v_{max} and K_m values) under the different conditions tested, we developed a simple mechanistic model for the pump cycle, shown in Scheme 1.

In this cycle, cytosolic protons associate with the protein (H$_{cyt}$:Pump), are then transported to the vacuolar side (Pump:H$_{vac}$) under consumption of the energy provided by ATP hydrolysis, and dissociate there. In principle, this cycle can function also in the inverse direction (10). To prove that at least some of the rate constants k_1', k_2, k_2', k_3, and/or k_3' are pH-dependent, it was initially hypothesized that they are all pH-inde-

$$\begin{array}{ccccc} & & \text{ATP} & \rightarrow & \text{ADP + Pi} \\ & k_1 & & k_2 & k_3 \\ \text{Pump + c[H}_{cyt}\text{]} & \rightleftarrows & \text{H}_{cyt}\text{:Pump} & \rightleftarrows & \text{Pump:H}_{vac} \rightleftarrows \text{Pump + c[H}_{vac}\text{]} \\ & k_1' & & k_2' & k_3' \end{array}$$

SCHEME 1

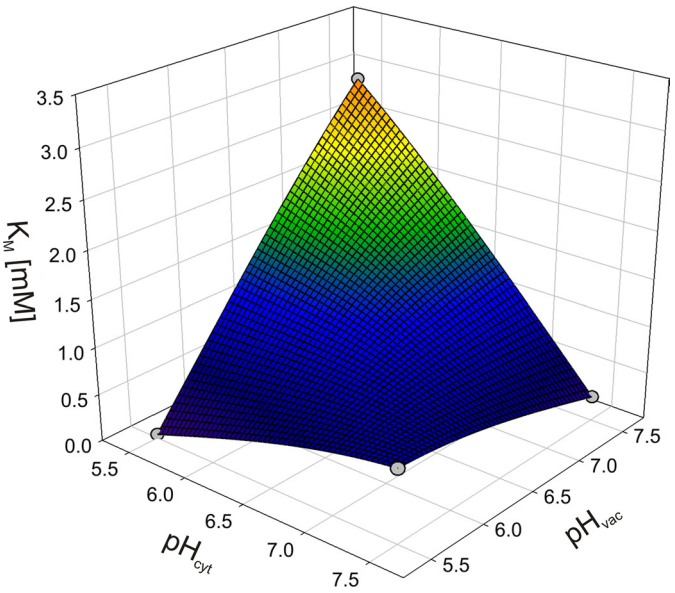

FIGURE 5. **pH dependence of K_m values for ATP of the vacuolar proton ATPase in a three-dimensional plot.** Data (*gray dots*) were obtained from fits with the Michaelis-Menten function to the data of Fig. 4. The spherical surface was superimposed to illustrate the locations of the data points in space.

pendent. This alternative hypothesis was confuted. It is shown that under this assumption, the different K_m values cannot be explained with this simple model.

In the conditions tested (especially $V = 0$ mV), the direction of proton flow is strongly biased in the cytosol → vacuole direction. Therefore, we considered only the case $k_2' = 0$. With this simplification, the proton current can be expressed as shown,

$$I = \frac{v_{max}[ATP]}{K_M + [ATP]} \quad \text{(Eq. 5)}$$

with

$$v_{max} = \text{const}\frac{(k_1[H_{cyt}])^c}{1 + \frac{(k_1[H_{cyt}])^c}{k_3} + \frac{(k_3'[H_{vac}])^c}{k_3}} \quad \text{(Eq. 6)}$$

and

$$K_M = \frac{k_1'k_3 + k_3(k_1[H_{cyt}])^c + k_1'(k_3'[H_{vac}])^c}{k_3 + (k_1[H_{cyt}])^c + (k_3'[H_{vac}])^c} \quad \text{(Eq. 7)}$$

Due to the limitation of the biological system to gain data points for more extreme conditions, it is not possible to reliably assign values to the free parameters of the model. However, the qualitative interpretation of the model allowed us to deduce far reaching hypotheses as outlined in the following. We first considered the experimental K_m values and plotted them for a better overview in a three-dimensional plot (Fig. 5), where the x and the y axis denote the cytosolic (pH_{cyt}) and the vaculor pH values (pH_{vac}), respectively. When starting with the physiological condition, pH_{cyt} 7.5/pH_{vac} 5.5, K_m = 0.8 mM, then an increase in the vacuolar pH to pH_{cyt} 7.5/pH_{vac} 7.5 results in a decrease of the K_m value. Assuming pH-independent constants in the model, such a reduction in K_m upon a decrease in [H_{vac}] can only be explained if $k_1' > k_3$ (for details, see the supplemental Appendix). Otherwise, the K_m would be constant ($k_1' = k_3$) or would increase ($k_1' < k_3$.) under the considered changes. However, a relation $k_1' > k_3$ would be contradictory to the observation upon a change from pH_{cyt} 5.5/pH_{vac} 5.5 to pH_{cyt} 5.5/pH_{vac} 7.5. It is observed that the K_m increases; but with $k_1' > k_3$ it would be predicted to decrease (see supplemental Appendix). Thus, the initial assumption that all constants are pH-independent is confuted. The whole set of data could be explained qualitatively if k_1' decreases upon a drop of pH_{cyt} (and/or k_1 increases), whereas k_3 increases upon an increase of pH_{vac} (and/or k_3' decreases). Physiologically, the change in k_1' (k_1) and k_3 (k_3') following pH_{cyt} and pH_{vac} changes would have a reasonable meaning: the pump protein would sense the cytosolic and the vacuolar pH, *e.g.* by protonation of the protein. The dissociation of the transported protons from the pump would be larger if the surrounding pH is high and smaller if the surrounding pH is low.

DISCUSSION

As outlined in this study, the vacuolar proton ATPase has peculiar features. Unlike the plant plasma membrane ATPase, which strongly hyperpolarizes the membrane (33, 34), the proton-pumping activity of the V-ATPase does not result in a strong hyperpolarization of the vacuolar membrane (Fig. 1*B*, *cf.* Refs. 7 and 8), indicating that the energy from the hydrolysis of one ATP molecule is used to transport several protons from the cytosol to the vacuole. This coupling is larger than the 1:1 stoichiometry of plasma membrane ATPases (for review, see Ref. 35) and very likely reflects the evolutionary origin of V-ATPases from an ATP synthase. A drawback of such a strong coupling, however, is that even small electrical gradients negatively interfere with pump activity. Consequently, V-ATPases can only establish larger pH gradients if the electrical gradient generated due to the charge transport dissipates immediately either by a shunt pathway or by other transporters harvesting this energy for their own use. This dissipation might be accomplished by a cation efflux from the vacuole or by an anion influx (36 and references therein and Ref. 37). So far, there are no indications that the V-ATPase itself mediates such a countertransport. However, we know that several electrogenic transporters like voltage-independent K^+ channels or the slow vacuolar channel TPC1 are dominating the electrical properties of the vacuolar membrane (36). Thus, we propose that the V-ATPase is acting in a fine-tuned concert with these transporters.

Another observation from the voltage dependence of the V-ATPase is the apparent pH dependence of the reversal voltage pointing to a pH-dependent H^+/ATP coupling ratio of this H^+ pump (Fig. 2). Reports on V-ATPases from *Saccharomyces cerevisiae, Beta vulgaris*, and *Citrus limon* also claimed variable coupling rates (17, 18, 28) From a structural point of view, a pH-dependent, flexible coupling ratio of the vacuolar H^+ ATPase is difficult to understand. However, if we assume the possibility, that dissociation of all bound protons from the c-ring is not mandatory for proper rotation of the pumping machinery, the observed effects could be explained. In the case of a neutral vacuolar pH, all protons tend to dissociate easily from the pump and thus the proton transport rate per hydrolyzed ATP molecule would be relatively high. With increasing

proton concentration in the vacuolar lumen, dissociation from the c-ring is less favored, and the rotary machinery may slip without releasing all protons into the vacuole (38, supplemental Appendix). Such a scenario would explain the reduced coupling ratio with decreasing vacuolar pH values (Fig. 2*B*). We have indications for such a scenario. A minimal model of the pH dependence of K_m values (Fig. 5) suggests that increasing proton concentrations at either side reduces the dissociation of protons from the pump (39).

A further inspection of the recorded pH dependences indicated a possibly even more complex regulation of the V-ATPase by cytosolic and vacuolar pH. As long as the pH on the cytosolic side was kept in the physiological range, *i.e.* at pH 7.5, changes in vacuolar pH had relative little effects on v_{max} and K_m (Fig. 4), whereas the coupling ratio decreased by 25% for a one pH unit acidification of the vacuole. After acidifying the cytosolic side to pH 5.5, in contrast, changes in vacuolar pH had a tremendous effect on v_{max} and K_m (Fig. 4). These results indicate that the cytosolic pH controls whether vacuolar pH changes have much of an effect on V-ATPase function or not. Moreover, it is unexpected that changes in vacuolar pH can have a more dramatic effect on the binding affinity of the cytosolic ATP-binding site of the V-ATPase than cytosolic pH changes have (Fig. 4). These results indicate that pH changes on either side of the vacuolar membrane affect the entire membrane-spanning V-ATPase and are thereby transferred to the other side of the membrane. Cytosolic pH controls the effects that vacuolar pH changes have, and, the other way around, vacuolar pH changes affect the ATP-binding site, which is on the other side of the membrane ~10 nm away. In this context, it is interesting that lysosomal V-ATPase in human cells has been shown recently to signal amino acid accumulation inside the lysosome to the outside (40).

In conclusion, we provided evidence here that the prevailing proton concentration on both sides of the membrane feeds back on the function of the V-ATPase. In fact, this feedback fine-tunes the protein to act in a most efficient way and guarantees that the ATPase is not accidentally converted by the physiological conditions into an ATP synthase. If the proton gradient is low, the pump might act at its limit and transport as many protons as possible. If the gradient, however, becomes larger, the pump would increasingly face the risk to act in an inverted way. A pH-dependent reduced dissociation from the c-ring would eliminate this problem. The pH-tuned action of the V-ATPase could then be compared with a car. On level ground, a high gear can be used to accelerate the car and to keep the speed. Uphill, however, the car keeps running in a smaller gear only.

Acknowledgments—We thank W. Junge and H. Wieczorek for helpful discussion.

REFERENCES

1. Okuno, D., Iino, R., and Noji, H. (2011) Rotation and structure of F_oF_1-ATP synthase. *J. Biochem.* **149,** 655–664
2. Cross, R. L., and Taiz, L. (1990) Gene duplication as a means for altering H^+/ATP ratios during the evolution of F_oF_1 ATPases and synthases. *FEBS Lett.* **259,** 227–229
3. Junge, W., Sielaff, H., and Engelbrecht, S. (2009) Torque generation and elastic power transmission in the rotary F_oF_1-ATPase. *Nature* **459,** 364–370
4. Cross, R. L., and Müller, V. (2004) The evolution of A-, F-, and V-type ATP synthases and ATPases: Reversals in function and changes in the H^+/ATP coupling ratio. *FEBS Lett.* **576,** 1–4
5. Klenk, H. P., Clayton, R. A., Tomb, J. F., White, O., Nelson, K. E., Ketchum, K. A., Dodson, R. J., Gwinn, M., Hickey, E. K., Peterson, J. D., Richardson, D. L., Kerlavage, A. R., Graham, D. E., Kyrpides, N. C., Fleischmann, R. D., Quackenbush, J., Lee, N. H., Sutton, G. G., Gill, S., Kirkness, E. F., Dougherty, B. A., McKenney, K., Adams, M. D., Loftus, B., Peterson, S., Reich, C. I., McNeil, L. K., Badger, J. H., Glodek, A., Zhou, L., Overbeek, R., Gocayne, J. D., Weidman, J. F., McDonald, L., Utterback, T., Cotton, M. D., Spriggs, T., Artiach, P., Kaine, B. P., Sykes, S. M., Sadow, P. W., D'Andrea, K. P., Bowman, C., Fujii, C., Garland, S. A., Mason, T. M., Olsen, G. J., Fraser, C. M., Smith, H. O., Woese, C. R., and Venter, J. C. (1997) The complete genome sequence of the hyperthermophilic, sulphate-reducing archaeon *Archaeoglobus fulgidus*. *Nature* **390,** 364–370
6. Ruppert, C., Schmid, R., Hedderich, R., and Müller, V. (2001) Selective extraction of subunit D of the Na^+-translocating methyltransferase and subunit c of the A_1A_0-ATPase from the cytoplasmic membrane of methanogenic archaea by chloroform/methanol and characterization of subunit c of *Methanothermobacter thermoautotrophicus* as a 16-kDa proteolipid. *FEMS Microbiol. Lett.* **195,** 47–51
7. Bethmann, B., Thaler, M., Simonis, W., and Schonknecht, G. (1995) Electrochemical potential gradients of H^+, K^+, Ca^{2+}, and Cl^- across the tonoplast of the green alga *Eremosphaera Viridis*. *Plant Physiol.* **109,** 1317–1326
8. Walker, D. J., Leigh, R. A., and Miller, A. J. (1996) Potassium homeostasis in vacuolate plant cells. *Proc. Natl. Acad. Sci. U.S.A.* **93,** 10510–10514
9. Schulz, A., Beyhl, D., Marten, I., Wormit, A., Neuhaus, E., Poschet, G., Büttner, M., Schneider, S., Sauer, N., and Hedrich, R. (2011) Proton-driven sucrose symport and antiport are provided by the vacuolar transporters SUC4 and TMT1/2. *Plant J.* **68,** 129–136
10. Gambale, F., Albert Kolb, H. A., Cantù, A. M., and Hedrich, R. (1994) The voltage-dependent H^+-ATPase of the sugar beet vacuole is reversible. *Eur. Biophys. J.* **22,** 399–403
11. Yokoyama, K., Muneyuki, E., Amano, T., Mizutani, S., Yoshida, M., Ishida, M., and Ohkuma, S. (1998) V-ATPase of *Thermus thermophilus* is inactivated during ATP hydrolysis but can synthesize ATP. *J. Biol. Chem.* **273,** 20504–20510
12. Hirata, T., Nakamura, N., Omote, H., Wada, Y., and Futai, M. (2000) Regulation and reversibility of vacuolar H^+-ATPase. *J. Biol. Chem.* **275,** 386–389
13. Beyhl, D., Hörtensteiner, S., Martinoia, E., Farmer, E. E., Fromm, J., Marten, I., and Hedrich, R. (2009) The fou2 mutation in the major vacuolar cation channel TPC1 confers tolerance to inhibitory luminal calcium. *Plant J.* **58,** 715–23
14. Bertl, A., Blumwald, E., Coronado, R., Eisenberg, R., Findlay, G., Gradmann, D., Hille, B., Köhler, K., Kolb, H. A., and MacRobbie, E. (1992) Electrical measurements on endomembranes. *Science* **258,** 873–874
15. Ivashikina, N., and Hedrich, R. (2005) K^+ currents through SV-type vacuolar channels are sensitive to elevated luminal sodium levels. *Plant J.* **41,** 606–14
16. Neher, E. (1992) Correction for liquid junction potentials in patch clamp experiments. *Methods Enzymol.* **207,** 123–131
17. Davies, J. M., Hunt, I., and Sanders, D. (1994) Vacuolar H^+-pumping ATPase variable transport coupling ratio controlled by pH. *Proc. Natl. Acad. Sci. U.S.A.* **91,** 8547–8551
18. Kettner, C., Bertl, A., Obermeyer, G., Slayman, C., and Bihler, H. (2003) Electrophysiological analysis of the yeast V-type proton pump: Variable coupling ratio and proton shunt. *Biophys. J.* **85,** 3730–3788
19. Krebs, M., Beyhl, D., Görlich, E., Al-Rasheid, K. A., Marten, I., Stierhof, Y. D., Hedrich, R., and Schumacher, K. (2010) *Arabidopsis* V-ATPase activity at the tonoplast is required for efficient nutrient storage but not for sodium accumulation. *Proc. Natl. Acad. Sci. U.S.A.* **107,** 3251–3256
20. Schulz-Lessdorf, B., and Hedrich, R. (1995) Protons and calcium modulate SV-type channels in the vacuolar-lysosomal compartment-channel inter-

action with calmodulin inhibitors. *Planta* **197,** 655–671
21. Cipriano, D. J., Wang, Y., Bond, S., Hinton, A., Jefferies, K. C., Qi, J., and Forgac, M. (2008) Structure and regulation of vacuolar ATPases. *Biochim. Biophys. Acta* **1777,** 599–604
22. Schumacher, K., Vafeados, D., McCarthy, M., Sze, H., Wilkins, T., and Chory, J. (1999) The *Arabidopsis* det3 mutant reveals a central role for the vacuolar H^+-ATPase in plant growth and development. *Genes Dev.* **13,** 3259–3270
23. Bennett, A. B., and Spanswick, R. M. (1984) H-ATPase activity from storage tissue of *Beta vulgaris*: II. H/ATP stoichiometry of an anion-sensitive H-ATPase. *Plant Physiol.* **74,** 545–548
24. Guern, J., Mathieu, Y., Kurkdjian, A., Manigault, P., Manigault, J., Gillet, B., Beloeil, J. C., and Lallemand, J. Y. (1989) Regulation of vacuolar pH of plant cells: II. A P NMR study of the modifications of vacuolar pH in isolated vacuoles induced by proton pumping and cation/H exchanges. *Plant Physiol.* **89,** 27–36
25. Schmidt, A. L., and Briskin, D. P. (1993) Energy transduction in tonoplast vesicles from red beet (*Beta vulgaris* L.) storage tissue: H^+/substrate stoichiometries for the H^+-ATPase and H^+-PPase. *Arch. Biochem. Biophys.* **301,** 165–173
26. Müller, M. L., Jensen, M., and Taiz, L. (1999) The vacuolar H^+-ATPase of lemon fruits is regulated by variable H^+/ATP coupling and slip. *J. Biol. Chem.* **274,** 10706–10716
27. Yabe, I., Horiuchi, K., Nakahara, K., Hiyama, T., Yamanaka, T., Wang, P. C., Toda, K., Hirata, A., Ohsumi, Y., Hirata, R., Anraku, Y., and Kusaka, I. (1999) Patch clamp studies on V-type ATPase of vacuolar membrane of haploid *Saccharomyces cerevisiae*. Preparation and utilization of a giant cell containing a giant vacuole. *J. Biol. Chem.* **274,** 34903–34910
28. Müller, M. L., and Taiz, L. (2002) Regulation of the lemon fruit V-ATPase by variable stoichiometry and organic acids. *J. Membr. Biol.* **185,** 209–220
29. Peiter, E., Maathuis, F. J., Mills, L. N., Knight, H., Pelloux, J., Hetherington, A. M., and Sanders, D. (2005) The vacuolar Ca^{2+}-activated channel TPC1 regulates germination and stomatal movement. *Nature* **434,** 404–408
30. Dadacz-Narloch, B., Beyhl, D., Larisch, C., López-Sanjurjo, E. J., Reski, R., Kuchitsu, K., Müller, T. D., Becker, D., Schönknecht, G., and Hedrich, R. (2011) A novel calcium binding site in the slow vacuolar cation channel TPC1 senses luminal calcium levels. *Plant Cell* **23,** 2696–2707
31. Voelker, C., Gomez-Porras, J. L., Becker, D., Hamamoto, S., Uozumi, N., Gambale, F., Mueller-Roeber, B., Czempinski, K., and Dreyer, I. (2010) Roles of tandem-pore K^+ channels in plants–a puzzle still to be solved. *Plant Biol.* **12,** 56–63
32. Marcel, D., Müller, T., Hedrich, R., and Geiger, D. (2010) K^+ transport characteristics of the plasma membrane tandem pore channel TPK4 and pore chimeras with its vacuolar homologs. *FEBS Lett.* **584,** 2433–2439
33. Blatt, M. R. (1992) K^+ channels of stomatal guard cells. Characteristics of the inward rectifier and its control by pH. *J. Gen. Physiol.* **99,** 615–644
34. Lohse, G., and Hedrich, R. (1992) Characterization of the plasma-membrane H^+-ATPase from *Vicia faba* guard cells. *Planta* **188,** 206–214
35. Briskin, D. P., and Hanson, J. B. (1992) How does the plant plasma membrane H^+-ATPase pump protons? *J. Exp. Bot.* **43,** 269–289
36. Hedrich, R., and Marten, I. (2011) TPC1-SV channels gain shape. *Mol. Plant* **4,** 428–441
37. Meyer, S., Scholz-Starke, J., De Angeli, A., Kovermann, P., Burla, B., Gambale, F., and Martinoia, E. (2011) Malate transport by the vacuolar AtALMT6 channel in guard cells is subject to multiple regulation. *Plant J.* **67,** 247–257
38. Grabe, M., Wang, H., and Oster, G. (2000) The mechanochemistry of V-ATPase proton pumps. *Biophys. J.* **78,** 2798–2813
39. Rastogi, V. K., and Girvin, M. E. (1999) Structural changes linked to proton translocation by subunit c of the ATP synthase. *Nature* **402,** 263–268
40. Zoncu, R., Bar-Peled, L., Efeyan, A., Wang, S., Sancak, Y., and Sabatini, D. M. (2011) mTORC1 senses lysosomal amino acids through an inside-out mechanism that requires the vacuolar H^+-ATPase. *Science* **334,** 678–683